Available online at www.sciencedirect.com

ScienceDirect

Defence Technology 9 (2013) 80–84

www.elsevier.com/locate/dt

Fabrication and Testing of Metal Foil Planar Switch

Qing-xuan ZENG*, Jun-jun LV, Ming-yu LI

State Key Laboratory of Explosion Science and Technology, Beijing Institute of Technology, Beijing 100081, China

Received 15 August 2012; revised 25 October 2012; accepted 12 November 2012
Available online 31 October 2013

Abstract

A metal foil spark gap switch is fabricated by using the magnetron sputtering deposition technology and the standard microelectronic technology. The switch consists of two main electrodes and a trigger electrode. Stylus profiler is used to measure the distance between the main electrode and the trigger electrode. The discharge characteristics of the metal foil spark gap switch are discussed. The switch has short delay time and low time jitter. When it is fired by a conventional capacitive discharge unit (CDU), the firing circuit has low inductance and resistance. Because of its low profile structure, it can be easily integrated with the bridge foil used in a conventional exploding foil initiator system (EFIS).

Keywords: Metal foil; Spark gap switch; Firing circuit

1. Introduction

Exploding foil initiator system (EFIS) has excellent safety and reliability. It can be used in the case of intense radiation, high altitude electro-magnetic pulse and stray current [1,2]. EFIS has been widely used in military and non-military applications [3]. Since the conception of slapper detonator has been proposed by J. R. Stroud [4], the lower energy, lower volume and higher integration of EFI have been the research topics. In recent years, the low energy exploding foil initiator (LEEFI) system has become the major research field [5].

In the development process of EFI, the research focuses on discharge circuit, bridge foil, flyer and explosive [6]. Generally, a CDU of EFI is connected to a bridge foil through a triggered spark gap switch. When the switch is triggered, a short burst of large electrical current is generated in the circuit. The bridge foil is vaporized and the plasma with high temperature and high pressure is produced under the action of the electrical current. Then, the insensitive high explosive is detonated by high-velocity flyer which is driven by the plasma. The traditional triggered spark switch is a stereo, three-electrode, pressurized gas-filled switch. This type switch has been used in EFIs for many years [7].

In 2009, Baginski et al. designed a one-shot switch for high-power pulse applications [8]. The high-voltage electrode layers of the switch are mainly copper. The switch has a sandwich layer structure, and the arrangement of switch layers is (Cu–W)-(parylene)-(Ti–W–Ti–Cu–Au). A Schottky diode is mounted on the top electrode. When the Schottky diode is triggered successfully, a plasma is generated to result in the breakdown of parylene layer and the closure of switch. The switch can be made by using conventional microelectronic technique, and the monolithic construction makes the switch more robust, reliable and consistent. In this paper, a metal foil spark gap switch is proposed. The spark gap switch and bridge foil can be formed using the traditional microelectronic processing technology.

2. Fabrication of metal foil spark gap switch

Crystalline glass is used as substrate, and Discovery 635 magnetron sputtering apparatus is employed to coat a 4–5 μm

* Corresponding author.
E-mail address: zengqingxuan@263.net (Q.X. ZENG).
Peer review under responsibility of China Ordnance Society

ELSEVIER Production and hosting by Elsevier

2214-9147/$ - see front matter
http://dx.doi.org/10.1016/j.dt.2012.11.001

thick copper layer on the polished surface of the substrate. A layer of positive photoresist is coated on the copper film. Then the substrate is soft-baked and is exposed by using contact lithography. After the substrate is developed with tetramethyl ammonium hydroxide (TMAH) developer, the exposed copper is etched by etching solution. The etching solution is comprised of 10 ml H_2SO_4, 10 ml H_2O_2 and 100 ml deionized water. The final substrate is dried in a nitrogen jet and cut into multiple test pieces. The metal foil triggered spark gap switch is shown in Fig. 1. The switch has two main electrodes and a trigger electrode. Dektak 150 type stylus profiler is used to characterize the physical dimensions of the switch. The stylus scan route A (Fig. 1) is used to measure the shortest distance between the main electrodes, and the stylus scan route B (Fig. 1) is used to measure the width of the trigger electrode. Fig. 2 (a) and (b) show the key dimensions of the switch. Because the pattern of switch is obtained by using wet etching method, the isotropic etching process makes the slant angle of wall of pattern edge be 45°. The shortest distance between the main electrodes is 1.0 mm, and the width of the trigger electrode is 300 μm, and the thickness of the copper foil is 4.35 μm. The roughness of the copper foil surface is determined by the preparation process, and the roughness of the substrate surface is between 0.02 and 0.06 μm.

In our experiment, two switches with the main gap distance of 1.5 mm and 1.0 mm were designed.

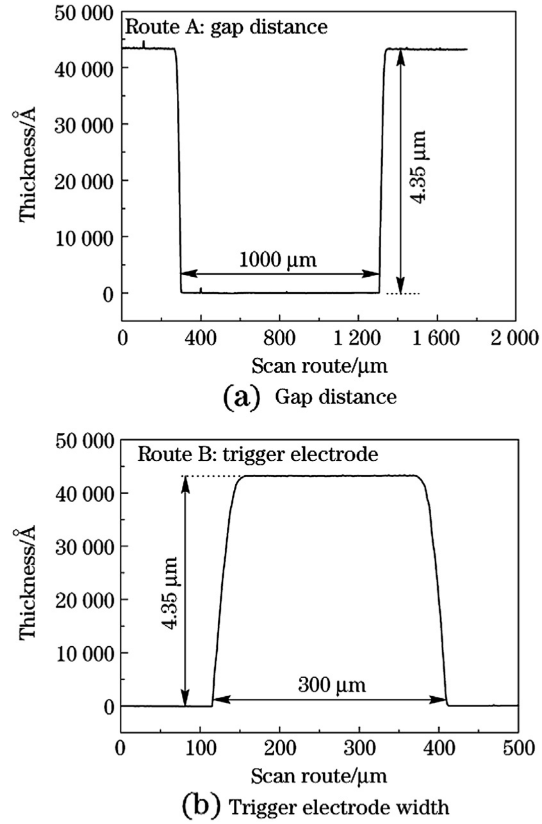

Fig. 2. Surface profile characterization of switch.

3. Self-breakdown voltage tests

As we know, the self-breakdown voltage (SBV) is a critical parameter of gas spark switch. It can be known from Paschen's law that the self-breakdown voltage of a gas gap is invariant if the gas pressure and the gap distance are constant. In general, the operating voltage of spark gap switch is not higher than 90 percent of its self-breakdown voltage. Therefore it is necessary to measure the self-breakdown voltage of the switch in stable atmosphere.

The self-breakdown voltage is defined as follows: two main electrodes are connected to the positive and negative poles of capacitor, respectively, the trigger electrode is connected to the adjacent negative electrode, and an increasing voltage is applied across the gas gap and the capacitor. When the voltage reaches the self-breakdown voltage of the gap, the gap would discharge the capacitor. DPO3054 oscillograph is employed to monitor the voltage drop waveforms of the main electrodes. In our experiment, a 0.22 μF capacitor is charged and the rate of the increasing voltage is about 6 V/s. The spark gap switches in the pressure containers with pure argon and nitrogen are tested, and the filling gas constant pressures are 0.5, 0.75, 1.0, 1.25, 1.5, 1.75 and 2.0 bars. When the gap is broken down, the self-breakdown voltage from voltage waveform is obtained. Then the above steps are repeated three times, and the recorded lowest voltage is the self-breakdown voltage of the spark gap switch. Fig. 3 shows a typical self-breakdown voltage waveform. The gap distance d is 1.5 mm, and the argon pressure is 1.5 bars in the container. When the voltage rises to 2060 V, the gas gap is punched through.

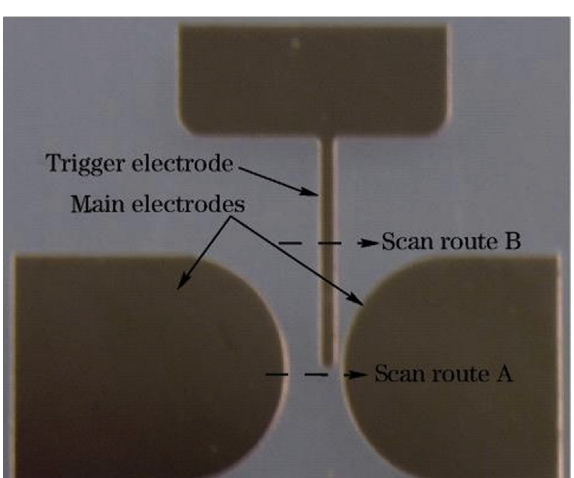

Fig. 1. Photograph of metal foil spark gap switch.

Paschen's law is used to characterize the breakdown voltage of a gas gap versus the product of gap distance and gas pressure. For a vacuum spark gap switch, it operates at a very low pressure; the Paschen's law is not applicable. And the breakdown voltage of the gap is determined by gap distance, electrode materials and so on. But the breakdown voltage of a gas spark gap switch is also determined by the gas pressure. The relations between the self-breakdown voltages of copper foil spark gaps and the product of gap distance and gas pressure are shown in Figs. 4 and 5, respectively. The result shows

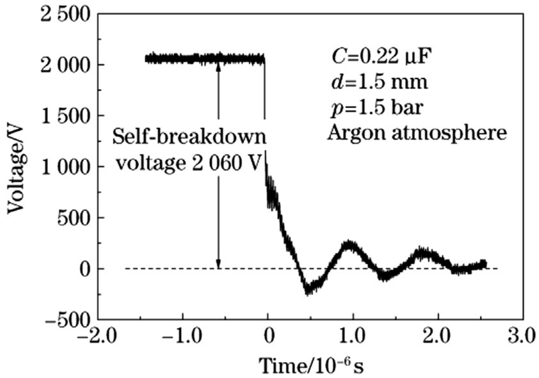

Fig. 3. A typical self-breakdown voltage waveform.

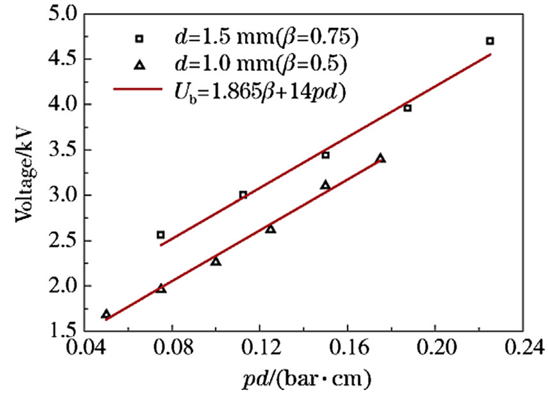

Fig. 5. Self-breakdown voltage vs. *pd* in nitrogen atmosphere.

that the self-breakdown voltage of switch is determined by the gas type, and the product of gas pressure and gap distance. When the product of gas pressure and gap distance increases, the self-breakdown voltage of gap increases. Because the first ionization energy of argon atom is lower, the breakdown of the gaps is easier when they work in argon atmosphere. According to the experimental results in Figs. 4 and 5, the relation between the self-breakdown voltage and the product of gap distance and gas pressure could be expressed as

$$U_b = A \cdot ß + B \cdot pd$$

where U_b is breakdown voltage, p is gas pressure and d is main gap distance, and β is geometric correction factor, which is determined by the material and geometry of electrode. β is estimated to be 0.75 (d = 1.5 mm) and 0.5 (d = 1.0 mm), respectively. Coefficients A and B are related to gas type. A and B are calculated to be 1.27 (1.865) and 4.9 (14) when the switch works in argon (nitrogen) atmosphere.

4. Delay time measurement

In general, the spark gap switch begins to work only when it is triggered at a desired time. Several methods, such as laser and field enhancement, can be used for triggering the spark gap switch. Before the gas gap is punched through, some primary electrons must be generated. In the experiment, when a triggering pulse voltage is applied to the trigger electrode, the gap between the trigger electrode and the adjacent main electrode is punched through to generate the initial charged particles. Some charged particles are accelerated under the action of strong electric field between the main electrodes. When the electrons gain sufficient energy which is greater than the ionization energy of the gas atoms, ionization would take place in the gas gap, and finally the main gap is punctured.

The spark gap switch is connected to a capacitor discharge circuit for testing, as shown in Fig. 6. A 0.22 μF capacitor is charged to a certain voltage. A short pulse trigger voltage (−1200V) which is applied between trigger electrode and ground of the circuit is used to initiate the breakover of the switch. DPO3054 oscillograph is employed to monitor the voltage waveform of the trigger electrode and the current waveform of the circuit. A high voltage probe (P6015A) is connected to Channel 1(ch1) to get the voltage waveform, and Rogowski coil current transformer is connected to Channel 2(ch2) to monitor the current waveform of circuit.

Fig. 7 shows a typical measurement result. Usually, the delay time is one of the most important parameters of spark gap switch. The delay time is defined as the time from applying a trigger voltage to the current appearing in the circuit, which is TD1 shown in Fig. 7. TD1 is an important parameter of a system including switch and trigger source. The

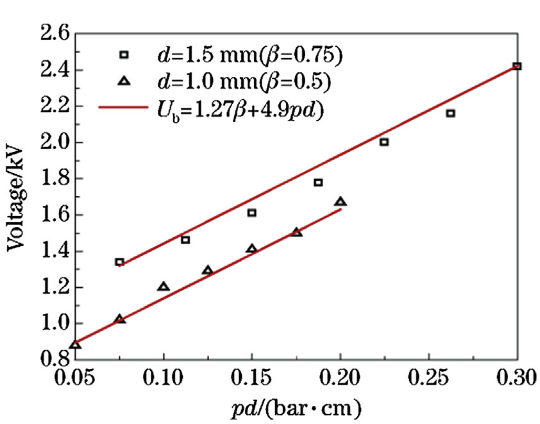

Fig. 4. Self-breakdown voltage vs. *pd* in argon atmosphere.

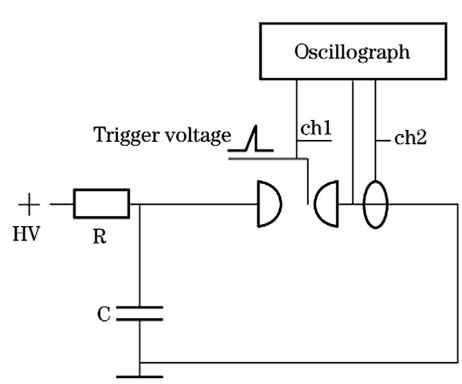

Fig. 6. Schematic diagram of discharge circuit of spark gap switch.

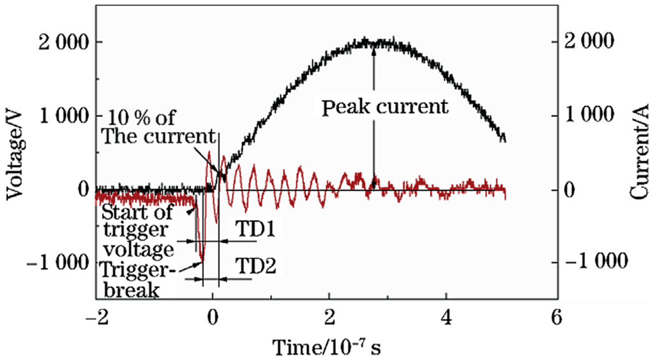

Fig. 7. Delay time.

time is determined by a trigger source which has a significant effect on TD1. So TD1 could not represent the timing precision of the switch. TD2 is defined as the switch time delay. TD2 is the time from trigger break to the start current of the circuit, as shown in Fig. 7.

The relations between TD2 and the operating voltages of spark gaps are shown in Figs. 8 and 9. Fig. 8 shows TD2 of spark gaps with distance between main electrodes of 1.5 mm, and Fig. 9 shows TD2 of spark gaps with distance between main electrodes of 1.0 mm. The two switches are tested in nitrogen atmosphere, and the pressure is 1.0 bar. It can be seen from Fig. 5 that SBVs of two spark gaps are 3440 V ($p \cdot d$ = 0.15 bar·cm) and 2260 V ($p \cdot d$ = 0.1 bar·cm), respectively. The operating voltage is selected in the range of 50% SBV to 90% SBV of the spark gaps. And the voltage intervals are 300 V and 200 V, respectively. At each voltage level, the experiment is repeated six times. The experimental results show that the delay time and time jitter depend on the applied voltage. It can be seen from Fig. 8 that, when the operating voltage reaches 3000 V (about 87% of SBV), the minimum TD2 is 8.8 ns; and the maximum TD2 is 13.6 ns. When the operating voltage is changed from 2400 V (about 70% of SBV) to 3000 V, TD2 is less than 24 ns. As the operating voltage is below 2400 V, TD2 increases steadily. So it's reasonable for the switch to work at voltage between 70% and 90% of its SBV.

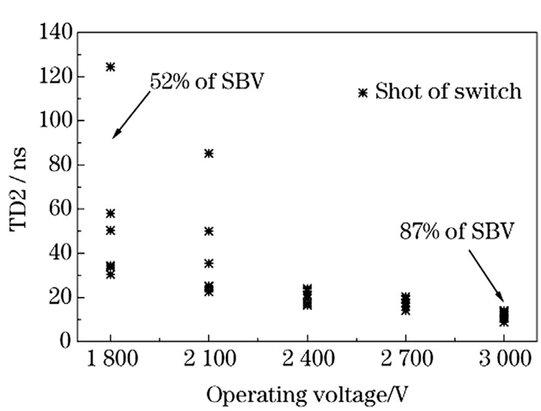

Fig. 8. TD2 versus operating voltage: the distance between the main electrodes is 1.5 mm.

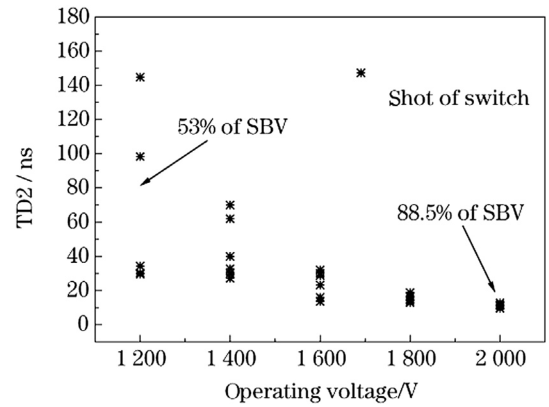

Fig. 9. TD2 versus operating voltage: the distance between the main electrodes is 1.0 mm.

It can be seen from Fig. 9 that, when the operating voltage reaches 2000 V (about 88.5% of SBV), the minimum TD2 is 9.6 ns, and the maximum TD2 is 12.8 ns. When the operating voltage is changed from 1600 V (about 70% of SBV) to 2000 V, TD2 is less than 30.2 ns. When it is below 1600 V, TD2 increases rapidly. So it's reasonable for switch to work at voltage between 70% and 90% of its SBV.

5. Inductance calculation

It is difficult to depict the complex breakdown process of an insulating medium (gas, liquid or solid). The capacitor discharge circuit shown in Fig. 6 is treated as a simple RLC circuit. In the circuit, C is the capacitor and the capacitance is 0.22 μF, L is the lumped inductance of the circuit which is comprised of the inductances of capacitor, wires, switch and all the soldering points, and R is the lumped resistance of the circuit which consists of equivalent series resistances of capacitor, switch and wires.

When L and R are treated as constants, the circuit can be described by Eq. (1)

$$\frac{1}{C}\int i dt + L\frac{di}{dt} + Ri = U_0, \tag{1}$$

where U_0 is the initial voltage of capacitor. Also the current can be calculated from Eq. (1)

$$i_{(t)} = \frac{U_0}{\omega L}\exp(-\delta t) \times \sin \omega t, \tag{2}$$

where

$$\delta = \frac{R}{2L}, \ \omega = \sqrt{\frac{1}{LC} - \frac{R^2}{4L^2}}.$$

The lumped R and L can be estimated form Eq. (2), which are expressed by Eqs. (3) and (4)

$$R = \frac{2L}{T_1}\ln\frac{I_{1\max}}{I_{2\max}}, \tag{3}$$

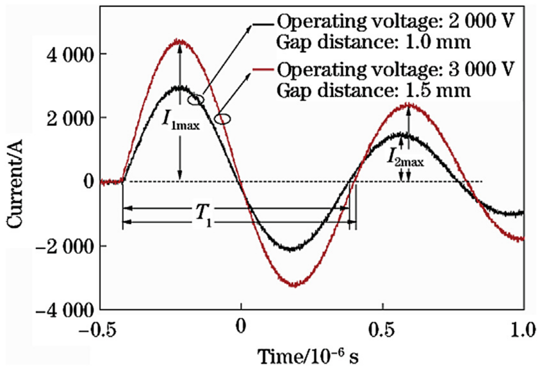

Fig. 10. Current waveforms of discharge circuit.

$$L = \frac{T_1^2}{C}\left[4\pi^2 + \left(\ln\frac{I_{1max}}{I_{2max}}\right)^2\right]^{-1}. \tag{4}$$

where I_{1max} is the first peak current value, I_{2max} is the second peak current value, and T_1 is the first discharging cycle of current waveform. All the three parameters can be obtained from the current waveform, as shown in Fig. 10.

Fig. 10 shows the current traces of the switch discharge circuit. The capacitor is charged to 3000 V when the spark gap between the main electrodes is 1.5 mm. And the capacitor is charged to 2000 V when the spark gap between the main electrodes is 1.0 mm. The first peak current value, the current rise time, the second peak current value and the first discharging cycle can be obtained from the current waveforms in Fig. 10. According to Eqs. (3) and (4), the lumped inductance and resistance are estimated to be 76.7 nH, 0.113 Ω ($d = 1.5$ mm) and 73.2 nH, 0.127 Ω ($d = 1.0$ mm), respectively. In the absence of a switch, the calculated inductance of the total circuit is 64.3 nH (±10%). Therefore the switch inductances of metal foil switches with different gaps are estimated to be 12.4 nH ($d = 1.5$ mm) and 8.9 nH ($d = 1.0$ mm), respectively.

The discharge properties of metal foil switch were compared with those of a commercial stereo switch. The parameters of I_{1max}, I_{2max}, T_1 and t_{1max} are listed in Table 1. The I_{1max} values of the two switches are comparative. The lumped inductance could be calculated from Eq. (4). The inductance of the metal switch is lower than that of commercial stereo switch. The time of first peak current t_{1max} and the first discharging cycle T_1 are shorter. In summary, the use of metal foil switch is beneficial to improve the energy utilization of EIFS (exploding foil initiator system).

Table 1
Calculated lumped inductance and resistance of circuit.

Switch type		Operating voltage/V	I_{1max}/A	I_{2max}/A	T_1/ns	L/nH	t_{1max}/ns
Metal foil	1.5 mm	3000	4400	2360	824	76.7	202
switch	1.0 mm	2000	2920	1480	806	73.2	202
Commercial stereo		3000	4445	3318	880	86.6	210
switch		2000	2960	2000	880	86.4	210

6. Conclusions

A metal foil spark gap switch was fabricated by using traditional microelectronic processing technology. The metal foil switch has stable static breakdown voltage. Its switch time delay can be as short as 8.8 ns. When it works in the capacitor discharging circuit, its inductance can be as low as 8.9 nH. Meanwhile, it can be used to replace the stereo, three-electrode and pressurized gas-filled switch.

References

[1] Zhou X, Shen RQ, Ye YH, Zhu P, Hu Y, Wu LZ. Influence of Al/CuO reactive multilayer films additives on exploding foil initiator. J Appl Phys 2011;110(09):1–6.
[2] Neyer Barry T, Adams JT, Edwards JC. Stouten- borough TL. A low cost, reliable, hermetically sealed, chip slapper detonator suitable for various aerospace applications. In: Proceedings of 35th Joint Propulsion Conference 1999.
[3] Ron Varosh. Electric Detonators: EBW and EFI. Propellants, Explosives, Pyrotechnics 1996;21:150–4.
[4] Stroud JR. A new kind of detonator-the slapper. UCRL-7739. Lawrence Livermore Laboratory report; 1976.
[5] McEntire RS, Butler P. Fuzing and firing systems at Sandia National Laboratories. In: 53rd Annual Fuze Conference 2009.
[6] Prinse WC, van't Hof, Cheng Lk, Schiltes JHG. High speed velocity measurements on an EFI-system. In: 27th International Congress on high-speed photography and photonics, Xi'an 2006.
[7] Chu KW, Scott GL. A comparison of high voltage switches. SAND99–0154. Sandia National Laboratories; 1999.
[8] Baginski TA, Thoma KA. A robust one-shot switch for high-power pulse applications. IEEE Trans Power Electron 2009;24(1):253–9.